Neuron, Volume *70*

Supplemental Information

Lhx6 and *Lhx8* Coordinately Induce Neuronal Expression of *Shh* that Controls the Generation of Interneuron Progenitors

Pierre Flandin, Yangu Zhao, Daniel Vogt, Juhee Jeong, Jason Long, Gregory Potter, Heiner Westphal, and John L.R. Rubenstein

Inventory of Supplemental Information

Supplemental data

Supplemental Figure Legends

Supplemental Experimental Procedures

Supplemental data

Figure S1, related to Figure 1:

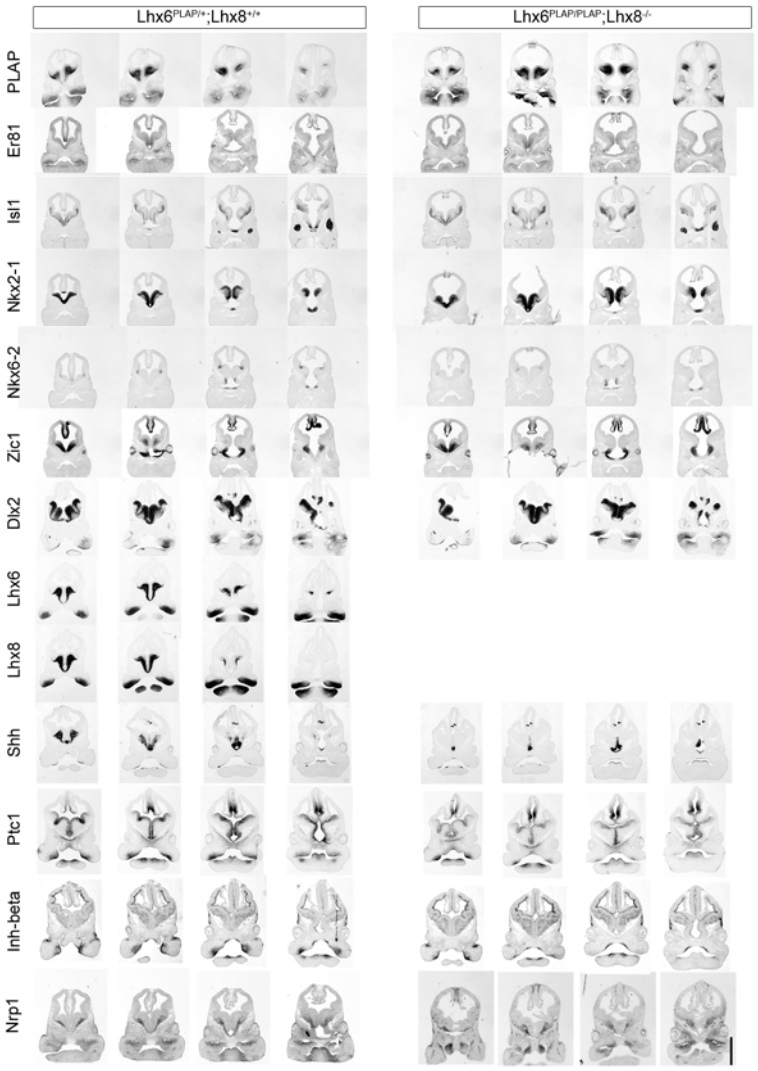

Figure S2, related to Figure 2:

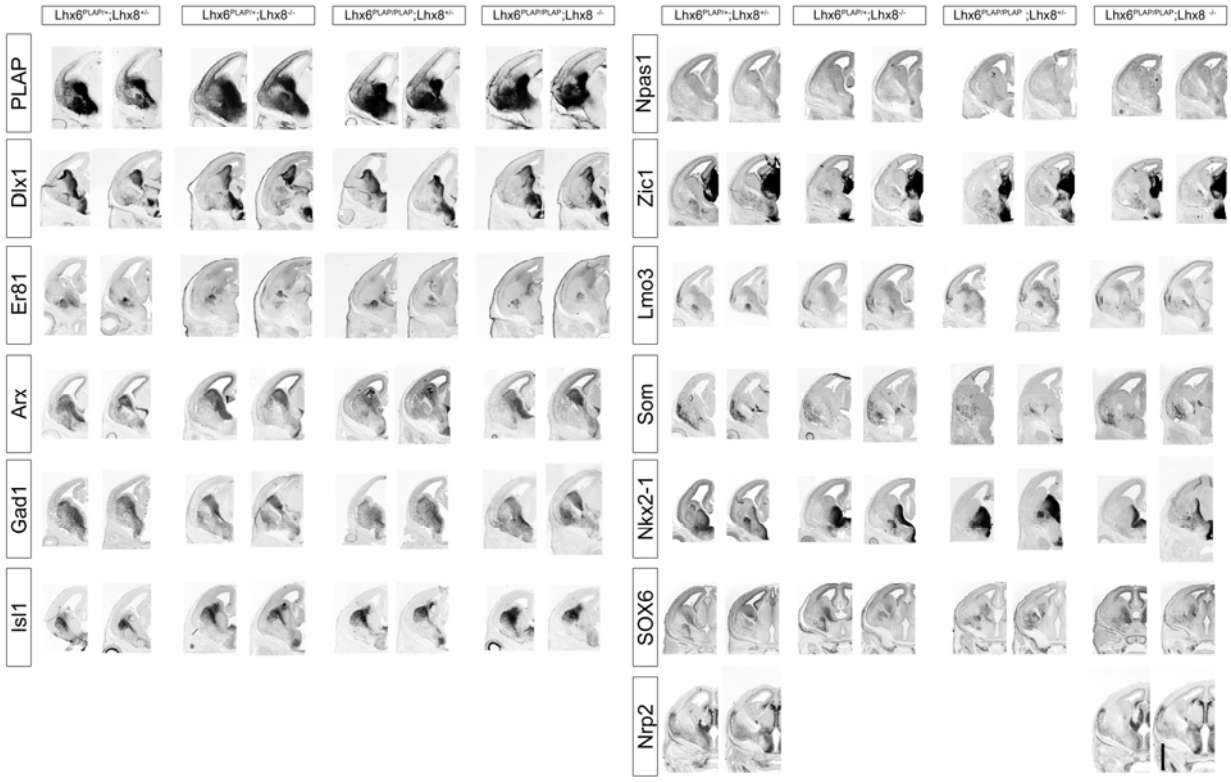

Figure S3, related to Figure 3:

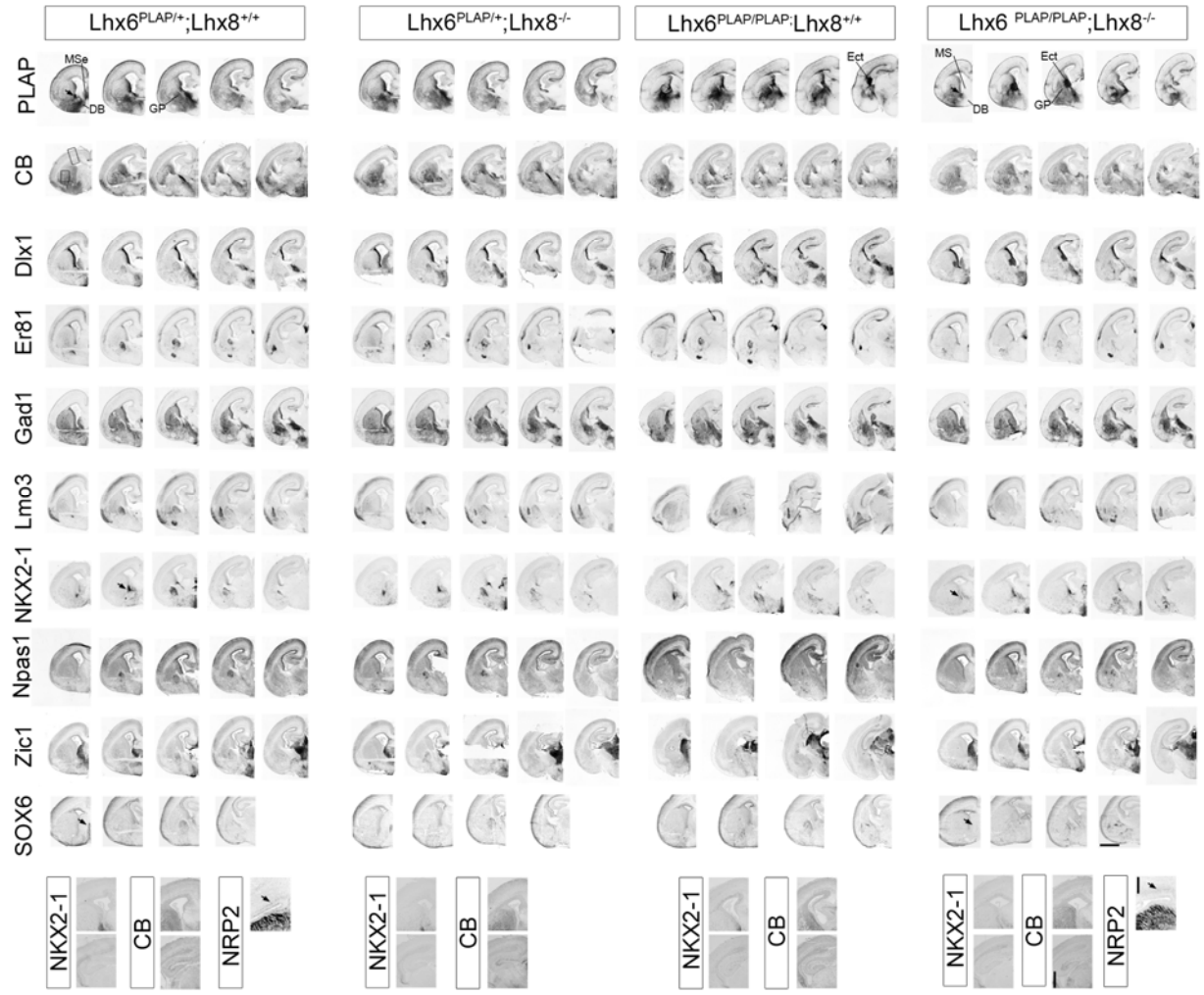

Figure S4, related to Figure 4:

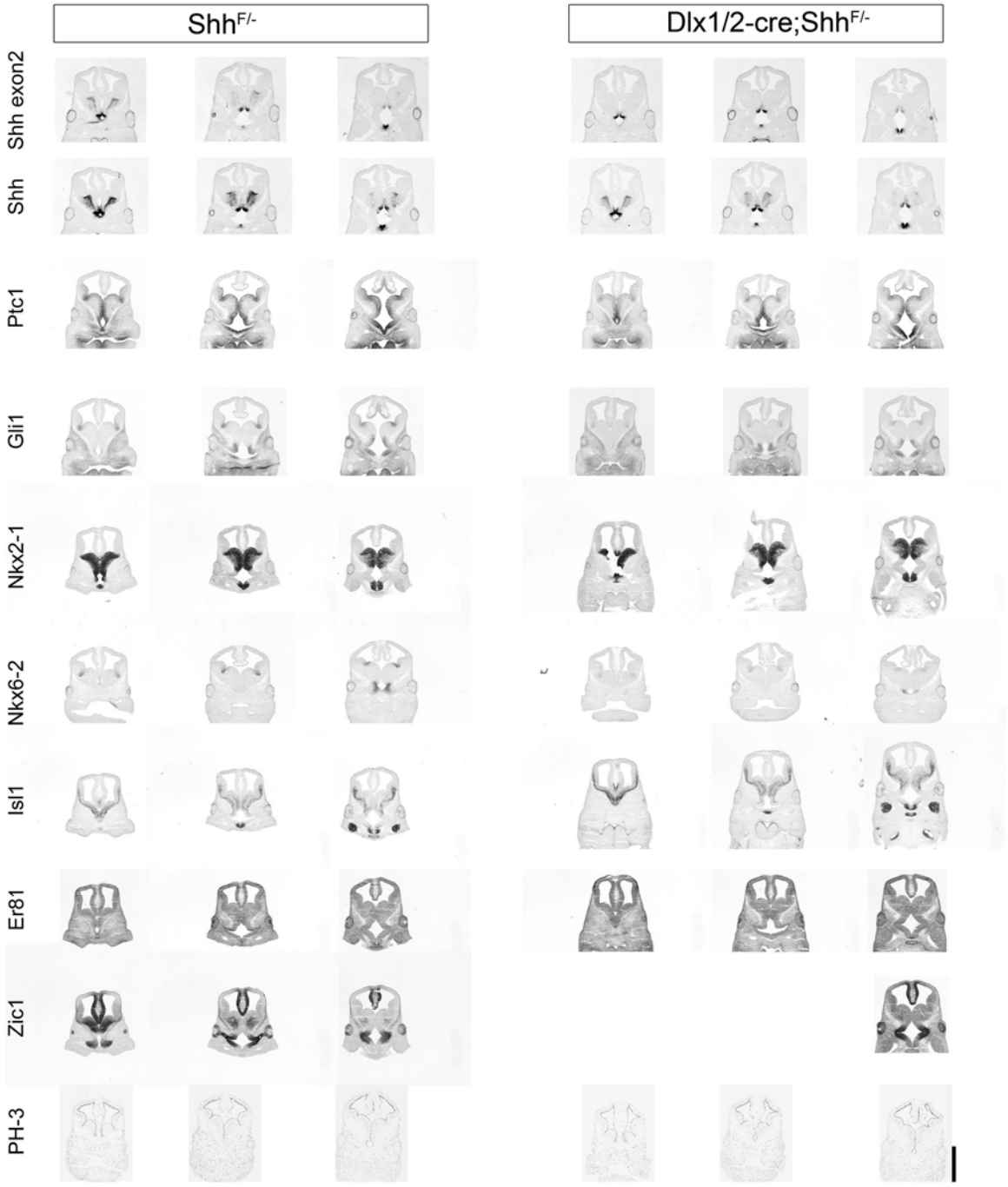

Figure S5, related to Figure 5:

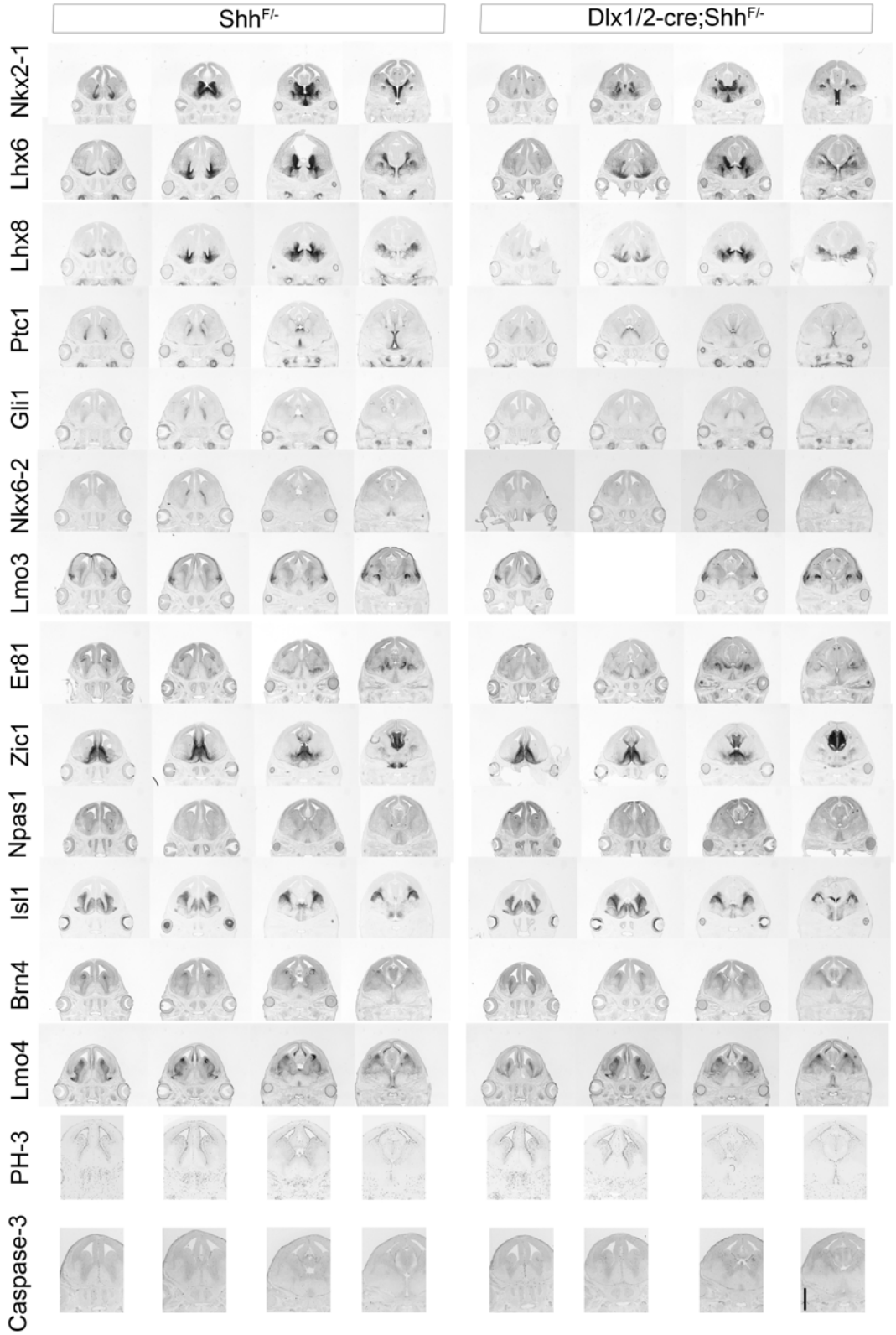

Figure S6, related to Figure 6:

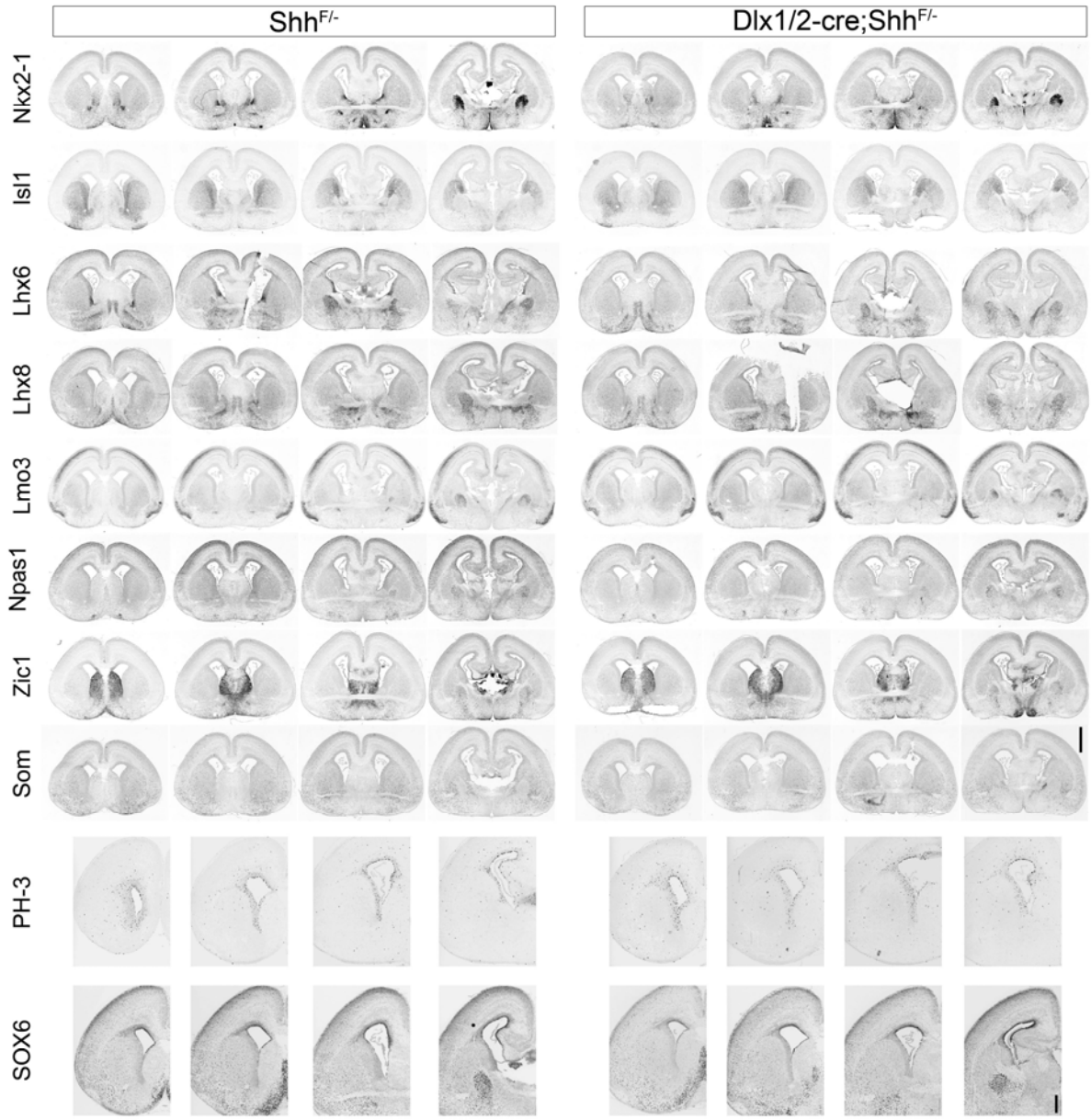

Table S1: related to figures 1 and 4 and Sup. Figs. S1 and S4.

	Control	$Lhx6^{PLAP/PLAP};Lhx8^{-/-}$	$Dlx1/2\text{-}Cre;Shh^{F/-}$
Ptc1	1	0.49	0.52
Nkx6-2	1	0.45	0.62

Table S2: related to figures 2 and 3 and Sup. Figs 2 and 3.

	STRIATUM			
	$Lhx6^{PLAP/+}$	$Lhx8^{-/-}$	$Lhx6^{PLAP/PLAP}$	$Lhx6^{PLAP/PLAP};Lhx8^{-/-}$
NKX2-1	139	170	155	82
Npas1	45	58		41
NPY	100	134	34	4
PLAP	354	413	292	286
SOM	63	92	46	30
SOX6	92	118	76	58

	CORTEX			
	$Lhx6^{PLAP/+}$	$Lhx8^{-/-}$	$Lhx6^{PLAP/PLAP}$	$Lhx6^{PLAP/PLAP};Lhx8^{-/-}$
Dlx1 svz	186	163	199	210
Dlx1 deep	319	255	344	270
Dlx1 sup.	135	205	194	69
Npas1 svz	80	70	44	69
Npas1 deep	196	166	105	175
Npas1 sup.	172	170	92	89
SOX6 svz	46	39	12	26
SOX6 deep	99	77	34	45
SOX6 sup.	248	250	26	33

Table S3: related to figures 5, 6 and 7 and Sup. Figs 5 and 6.

E14.0	**CORTEX**		
		$Shh^{F/-}$	$Dlx1/2\text{-}cre;Shh^{F/-}$
	CB MZ	34	33
	CB CP/IZ	17	13
	CB SVZ	63	53
	Lhx6 MZ	37	33
	Lhx6 CP/IZ	30	20
	Lhx6 SVZ	96	85
E18.5	**STRIATUM**		
		$Shh^{F/-}$	$Dlx1/2\text{-}cre;Shh^{F/-}$
	Lhx6	146	128
	Lhx8	107	112
	NKX2-1	150	125
	Som	174	117
	SOX6	149	136
	LGE		
		$Shh^{F/-}$	$Dlx1/2\text{-}cre;Shh^{F/-}$
	Lhx6 LGE svz	84	38
	NKX2-1 LGE svz	53	15
	CORTEX		
		$Shh^{F/-}$	$Dlx1/2\text{-}cre;Shh^{F/-}$
	CB svz	29.2	12.8
	CB deep	35.2	12.6
	CB sup.	76.8	39.8
	Lhx6 svz	64	20
	Lhx6 deep	66	27
	Lhx6 sup.	158	75
	Npas1 svz	41	26
	Npas1 deep	43	29
	Npas1 sup.	108	96
	Som svz	4	2
	Som deep	8	5
	Som sup.	22	11
	SOX6 svz	38	24
	SOX6 deep	148	118
	SOX6 sup.	382	295

	STRIATUM			
		% Change (MUT/HET*100)	sem	paired T-test
P24	PV	85	2	0.01
	SOM	90	8	0.29
	CR	89	3	0.30
	NPY	114	4	0.09

Supplemental Figure Legends

Figure S1 related to Figure 1:

In situ RNA hybridization analysis of gene expression in E11.5 *Lhx6*$^{PLAP/PLAP}$*;Lhx8*$^{-/-}$ double mutant and *Lhx6*$^{PLAP/+}$*;Lhx8*$^{+/+}$ controls. Four serial coronal sections through the head (rostral-most on the left) show expression of PLAP (from the *Lhx6* allele by histochemistry), *ER81, Isl1, Nkx2-1, Nkx6-2, Zic1, Dlx2, Lhx6, Lhx8, Shh, Ptc1, Inh-beta,* and *Neuropilin-1*. Scale bar: 1 mm.

Figure S2 related to Figure 2:

In situ RNA hybridization, PLAP staining and immunohistochemistry analysis at E14.5 in the following genotypes: *Lhx6*$^{PLAP/+}$*;Lhx8*$^{+/+}$*, Lhx6*$^{PLAP/+}$*;Lhx8*$^{-/-}$*; Lhx6*$^{PLAP/PLAP}$*;Lhx8*$^{+/-}$ and *Lhx6*$^{PLAP/PLAP}$*;Lhx8*$^{-/-}$. Two serial coronal hemisections through the head (rostral-most on the left) show expression of PLAP (from the Lhx6 allele by histochemistry), *Dlx1, ER81*, *Arx, Gad1, Isl1, Npas1, Zic1, Lmo3, Som, Nkx2-1,* SOX6 (immunohistochemistry) and *Neuropilin-2*. Scale bar: 1 mm.

Figure S3 related to Figure 3:

Gene expression analysis at E18.5 in the following genotypes: *Lhx6*$^{PLAP/+}$*;Lhx8*$^{+/+}$*, Lhx6*$^{PLAP/+}$*;Lhx8*$^{-/-}$*; Lhx6*$^{PLAP/PLAP}$*;Lhx8*$^{+/+}$ and *Lhx6*$^{PLAP/PLAP}$*;Lhx8*$^{-/-}$*.* **Top**: Analysis of four/five serial coronal hemisections through the brain (rostral-most on the left) show expression of PLAP (from the Lhx6 allele by histochemistry), Calbindin (CB; immunohistochemistry), *Dlx1, ER81, Gad1, Lmo3, NKX2-1* (immunohistochemistry; note: the third genotype is *Lhx6*$^{PLAP/PLAP}$; *Lhx8*$^{+/-}$*), Npas1, Zic1*, and SOX6

(immunohistochemistry). **Bottom**: Selected higher magnification views of immunohistochemistry of the cortex and hippocampus are shown for NKX2-1, Calbindin and Neuropilin-2. Arrows in NRP2 panels indicates the $NRP2^{+}$ cells in the neocortex SVZ. Abbreviations: Ect: ectopia; DB: diagonal band; GP: globus pallidus; MSe: medial septum. Scale bar: 1mm (in SOX6 right-most panel) for PLAP to SOX6 panels; 400 µm (in CB right-most panel; bottom one) for NKX2-1 and CB immunostaining; 100 µm for NRP2 immunostaining.

Figure S4 related to Figure 4:

In situ RNA hybridization analysis of gene expression in E11.5 control ($Shh^{F/-}$) and *Shh* conditional mutant (*Dlx1/2-cre;*$Shh^{F/-}$). Three serial coronal sections (rostral-most on the left) show expression of *Shh exon 2*, *Shh* (homologous to coding region), *Ptc1, Gli1, Nkx2-1, Nkx6-2, Isl1, ER81* and *Zic1*. PH3 immunostaining is shown in the bottom-most row. Scale bar: 1 mm.

Figure S5 related to Figure 5:

Top: In situ RNA hybridization analysis of gene expression in E14.0 control ($Shh^{F/-}$) and *Shh* conditional mutant (*Dlx1/2-cre;*$Shh^{F/-}$). Four serial coronal sections (rostral-most on the left) show expression of *Nkx2-1, Lhx6, Lhx8, Ptc1, Gli1, Nkx6-2, Lmo3, ER81, Zic1, Npas1, Isl1, Brn4* and *Lmo4.* **Bottom**: Immunostaining for PH3 and activated Caspase-

3 expression on coronal hemisections through the brain (rostral-most on the left). Scale bar: 1 mm.

Figure S6 related to Figure 6:

In situ RNA hybridization and immunohistochemistry analysis in E18.5 control (*Shh*$^{F/-}$) and *Shh* conditional mutant (*Dlx1/2-cre;Shh*$^{F/-}$). Four serial coronal sections (rostral-most on the left) show expression of *Nkx2-1, Isl1, Lhx6, Lhx8, Lmo3, Npas1, Zic1*, *Som* and immunostaining for PH3 and SOX6. Scale bar: 1mm (in Som right-most panel) for *in situ* hybridization panels (Nkx2-1 to Som); 400 µm (in SOX6 right-most panel) for PH3 and SOX6 immunostaining (2 rows of panels at the bottom).

Table S1: Table showing the relative RNA expression (dorsal MGE compared to the POA) of Ptc1 and Nkx6-2 in controls and two different mutants (Lhx6 $^{PLAP/PLAP}$;Lhx8$^{-/-}$; conditional Shh mutant (Dlx1/2-cre). RNA in situ hybridization of E11.5 with both Ptc1 and Nkx6-2 are showed in Figure 1 for the Lhx6&8 double mutant and in Figure 4 for the Shh conditional mutant. Both Lhx6&8 and Shh conditional mutants have ~ 50% decrease in the RNA expression of Ptc1 and Nkx6-2 in the dorsal MGE. Identical square area (~800 pix^2) was designed in the dMGE and the POA from the ISH images for both genotypes. Average pixel intensity from these regions was determined using the histogram function of ImageJ software (http://rsbweb.nih.gov/ij/). The signal intensity

of the dorsal MGE was normalized by the signal intensity from the POA for each gene and each genotype. (Related to figures 1 and 2 and Sup. Figs. S1 and S4).

Table S2: Quantification of number of cortical and striatal interneurons in the *Lhx6*$^{PLAP/+}$, *Lhx8*$^{-/-}$, *Lhx6*$^{PLAP/PLAP}$ *and Lhx6*$^{PLAP/PLAP}$*;Lhx8*$^{-/-}$ at E18.5 (Related to Figs. 2 and 3 and Sup. Figs 2 and 3).

Table S3: Quantification of number of cortical and striatal interneurons in the *Shh*$^{F/-}$ control and *Dlx1/2*-cre;*Shh*$^{F/-}$ mutant at E14.5, E18.5 and P24. The table for the P24 data shows percentage of change of striatal interneurons in the mutant compared to the control (mutant/control*100) (Related to Figs. 5, 6 and 7 and Sup. Figs 5 and 6).

Supplemental Experimental Procedures

Mice

Lhx6$^{+/PLAP}$ mice were provided by Regeneron; they were generated and genotyped according to Choi et al. (2005). *Lhx6*$^{+/PLAP}$ mice were crossed with *Lhx8*$^{+/-}$ mice (Zhao et al., 1999) to generate *Lhx6*$^{+/PLAP}$*;Lhx8*$^{+/-}$animals, which were crossed to generate control and mutant animals. The *Lhx8* wild-type allele was genotyped as described previously (Zhao et al., 1999). The *Lhx8* mutant allele was genotyped by PCR using the following primers: 5'-TGGCTGCTAGCGTGAAAGCACAA; 5'-TATCGCCTTGACGAGTTCTTCTGA. *Shh*$^{F/F}$ mice (Dassule et al., 2000) were crossed

with *Dlx1/2-cre* animals (Potter et al., 2009). The *Dlx1/2-cre* line has been shown to initiate recombination in the SVZ the MGE (Potter et al., 2009). *Dlx1/2-cre;Shh*$^{+/-}$ males were bred with *Shh*$^{F/F}$ females (Dassule et al., 2000) to generate control and mutant mice for analysis. Animals were treated in accordance with the protocols approved by the NICHD and UCSF Animal Use Committees.

Histology

Embryos were immersion fixed in 4% paraformaldehyde (PFA) in phosphate-buffered saline (PBS), pH 7.4 for 4–12 hours; postnatal animals were fixed by cardiac PFA perfusion; brains were postfixed overnight, cryoprotected in a gradient of sucrose to 30%, frozen in embedding medium (OCT, Tissue-Tek, Torrance, CA), and cut by using a cryostat (20 µm thick).

In situ RNA hybridization experiments were performed using digoxigenin riboprobes on 20 µm frozen sections as previously described (Cobos et al., 2007). All riboprobes were described in Long et al., 2009a, except for except for Ptc1 (Andy McMahon), and Shh exon 2 (amplified by PCR using the following primers: forward 5'AAGACAAGTTAAATGCCTTGGCC3' and reverse 5'TCACAGAACAGTGGATGTGAGC, and cloned between the HindIII and EcoRI sites of pBluescript).

Immunofluorescence staining was performed according to Flandin et al. (2010); cryostat sections were 20 µm on slides (for embryonic ages), or 40 µm free-floating (for postnatal ages) using the following antibodies: rabbit anti-BLBP (Chemicon, Temecula, CA, 1:1000); rabbit anti-calbindin (CB) (Chemicon, Temecula, CA, 1:1000); rabbit anti-calretinin (Swant, Bellinzona, Switzerland, 1:2000); rabbit anti- cleaved caspase3 (BD pharmingen,CA ,1:500); rabbit anti MAFb (Bethyl Laboratories, TX, 1:1000); mouse anti-Nestin (Chemicon, Temecula, CA, 1:1000); rabbit anti-Nkx2-1 (TTF-1) (Santa Cruz Biotechnology, Santa Cruz, CA, 1:1000); rabbit anti-NPY (ImmunoStar, Hudson, WI, 1:2000); goat anti-neuropilin-2 (R&D Systems, 1:500); mouse anti-parvalbumin (Swant, Bellinzona, Switzerland, 1:4000); rabbit anti-phospho-histone H3 (Upstate Biotechnology, Lake Placid, NY, 1:200); ; rat anti-somatostatin (Chemicon, Temecula, CA, 1:150); rabbit anti-Sox6 (Abcam, Cambridge, MA, 1:500); rabbit anti-phospho-histone H3 (Upstate Biotechnology, Lake Placid, NY, 1:200). Alexa 488 and 594 were used as secondary antibodies (Invitrogen). PLAP expression was assayed as in Shah et al. (2004).

Data collection and quantification

Brightfield images (PLAP staining and in situ hybridization) were taken by using an SZX7 microscope (Olympus, Japan) and DP70 camera (Olympus, Japan). Images were manipulated with Photoshop CS3 software (Adobe Systems, San Jose, CA). Contrast and brightness of these images were adjusted for better visualization.

For counting of striatal and cortical interneurons at E18.5 in the *Lhx6/ Lhx8* mutant, boxes were placed over images of the center of the striatum or in the somatosensory cortex of *Lhx6*$^{+/-}$*;Lhx8*$^{+/+}$ and *Lhx6*$^{-/-}$*;Lhx8*$^{-/-}$. 1-2 sections for each genotype were used for counting (see striatal and neocortical boxes in Sup. Fig. 3). We analyzed NKX2-1, NPY, SOM and SOX6 expression using immunohistochemistry and Lhx6-PLAP by histochemistry; in situ RNA hybridization was used for *Npas1* and *Dlx1*.

For counting cells in the striatum and LGE at E18.5 in the control and *Dlx1/2-cre;Shh*$^{F/-}$ mutant (Fig. 6), three sections were used and numbers were averaged. We analyzed NKX2-1 and SOX6 expression using immunohistochemistry; in situ RNA hybridization was used for the other markers (*Lhx6*, *Lhx8* and *Som*).

Phospho-histone H3 positive cells were counted at E15.5 and E18.5 in control and *Dlx1/2-cre;Shh*$^{F/-}$ mutant in the VZ and SVZ of the rostral MGE. The perimeter of the counting box was delimited the region of Nkx2-1 expression. A total of three brains for each genotype were used and two sections were counted for each brain; numbers were averaged.

Numbers of the subtypes of cortical interneuron (PV, NPY, SS and CR) were counted in the somatosensory cortex at P24 of the control and *Dlx1/2-cre;Shh*$^{F/-}$ mutant animals (Fig. 7). Counting boxes were designed that divided the cortical plate into the superficial layers (layer I to IV) and the deep layers (layer V and VI). We counted cells in these two

boxes for three different brains for each genotype. For each brain, three sections were counted and assessed using a two-tailed paired Student-test.

Plasmid Vectors: *Shh* Enhancer and Lhx6 and Lhx8 expression vectors

Shh Enhancer (SBE3) Luciferase and mCherry reporter vectors

The *Shh* SBE3 (ECR3) enhancer (384 bp) was PCR amplified from C57BL/6 mouse DNA using previously described primers (Jeong et al., 2006), that were modified to introduce KpnI and HindIII restriction sites on the 5' and 3' sites, respectively, and cloned into the PGL4.23 luciferase vector (Promega) (SBE3-Luciferase vector). The luciferase reporter was excised with HindIII and XbaI and replaced with mCherry to generate the SBE3-wtA-mCherry reporter vector.

Mutating putative LHX binding site in SBE3: The MatInspector software tool from Genomatix (http://www.genomatix.de) identified one Lim homeodomain binding site; LHX site A (34 to 56bp of the SBE3 enhancer: 5'- CCTGACAGATAATCAAGGCCTTA -3'; the core LHX binding sequence is underlined. Site-directed mutagenesis replaced the 6 nucleotide core sequence with TTTTTT, using the following primers:

SBE3-mutA forward:

5'– GATTTTACAGGCCTGACAGATTTTTTAGGCCTTATTATACTGGG -3',

and reverse:

5’- CCCAGTATAATAAGGCCTAAAAAATCTGTCAGGCCTGTAAAAC -3’,

The mutated SBE3 enhancer was cloned into KpnI and HindIII sites of the mCherry reporter plasmid to generate the SBE3-mutA-mCherry reporter vector.

All vectors were verified by sequencing.

Transcription factor expression vectors

The pCMV-IRES-EGFP expression vector was constructed by ligating the multiple cloning site-IRES-EGFP fragment of the pIRES2-EGFP vector (Clontech) into NheI and BsrGI restriction sites on the pSico backbone, (gift from Ramalho-Santos lab, UCSF) (Gaspar-Maia et al., 2009). The resulting vector contained a multiple cloning site downstream of the CMV promoter, as well as EGFP downstream of an IRES element. Human *Lhx6* (the forebrain enriched *Lhx6.1* isoform) (Kimura et al., 1999) was inserted into multiple cloning site of the pCMV-IRES-EGFP vector (into 5’ NheI and 3’ XmaI sites) to generate: pCMV-Lhx6-IRES-EGFP (pCMV-IRES-EGFP without Lhx6 was used as a control).

Human *Lhx8* coding sequence (Full length cDNA, Open Biosystems, cat # MHS1010-97227971) was amplified by PCR and cloned into NotI and KpnI sites of the p3xFLAG-CMV-10 expression vector (3xFLAG on the N terminal side; Sigma) to generate p3xFLAG-Lhx8-CMV-10 (p3xFLAG-CMV-10 vector without Lhx8 was used as a control).

Human Ldb1 coding sequence (isoform Ldb1-001; coding for 375 amino acids) was cloned into the EcoRI and XhoI sites of the pCAGGS/ES expression vector, to generate pCAGGS/ES-Ldb1.

All vectors were verified by sequencing.

Transcription activation assays in primary MGE cultures

The MGE (progenitor and mantle zones) was dissected from E12.5 CD-1 wild type embryos. The MGE was mechanically dissociated in N5 media (5% fetal bovine serum, 1x N2 supplement, 35 µg/ml bovine pituitary serum, 20 µg/ml basic FGF, 20 µg/ml EGF) (Scheffler et al., 2005) and cells seeded at a density of 2.5×10^5 cells per cm^2 in 8-well chamber slides (0.8 cm^2; Lab-Tek, Nalgene) coated with poly-L-lysine (10 µg/ml, Sigma) and laminin (5 µg/ml, Sigma).

Cells were grown in N5 media and transfected with 500 ng of total DNA 24 hours after seeding using Fugene6 (Roche). 48 hours after transfection the cells were fixed in 4% paraformaldehyde.

For Lhx6 transfections, we used:

166 ng of reporter (with SBE3-wtA or with SBE3-mutA); 166 ng of pCMV-Lhx6-IRES-EGFP; 166 ng of p3xFLAG-CMV-10.

For Lhx8 transfections, we used:
166 ng of reporter (with SBE3-wtA or with SBE3-mutA); 166 ng of p3xFLAG-Lhx8-CMV-10; 166 ng of pCMV-IRES-EGFP.

For Lhx6&8 transfections, we used:
166 ng of reporter (with SBE3-wtA or with SBE3-mutA); 166 ng of pCMV-Lhx6-IRES-EGFP; 166 ng of p3xFLAG-Lhx8-CMV-10.

Finally, for transfections without transcription factors we used:
166 ng of reporter (with SBE3-wtA or with SBE3-mutA); 166 ng of pCMV-IRES-EGFP; 166 ng of p3xFLAG-CMV-10.

Protein expression was detected by immunofluorescence: rabbit anti-DsRed (detects mCherry) (1/500, Clontech), chicken anti-GFP (1/1000, Aves Labs), and mouse anti-Neuronal Nuclei (NeuN; 1/1000, Millipore). Goat anti-rabbit Alexa 546, anti-chicken Alexa 488 and anti-mouse Alexa 647 were used as secondary antibodies (Invitrogen, 1:250).

To measure the number of $mCherry^+$ cells, 4x images were taken using a fluorescent microscope. Images were then studied using ImageJ software. We determined a

threshold to select the cells with the strongest mCherry intensity (50-100% maximum intensity). Then, we used “analyze particules” function (object size: 4 to infinity in pixel^2; circularity parameter were unchanged) to obtain the number of mCherry$^+$ cells. Four experiments were performed and the number of mCherry$^+$ cells was averaged for each condition.

The results were normalized to account for differences in transfection efficiency. The number of mCherry$^+$ cells was divided by the transfection efficiency factor. The transfection efficiency factor was calculated by dividing the number of GFP$^+$ cells (all experiments had an internal control of an expression vector driving GFP expression; see above) by the number of DAPI$^+$ cells. (Figure 8C). Error bars represent the standard error of the mean. The unpaired two-tailed Student t-test was used for the statistical analysis. *, $p<0.05$.

In a parallel set of analyses, we used the SBE3-luciferase reporter (instead of mCherry), and obtained similar results. Rabbit anti-firefly luciferase (1/1000, Abcam) was used to detect luciferase expression. Luciferase positive cells were counted for each condition and compared to the expression of luciferase driven by the *Shh* enhancer without any transcription factors (i.e. GFP alone). Data were analyzed from three independent experiments, with at least four replicates for each condition performed for each experiment (data not shown).

Electrophoretic mobility shift assay (EMSA)

EMSA were performed using the kit from Pierce. Briefly, each reaction (20µL) consisted of ~2 µg nuclear extract, in binding buffer consisting of: 10 mM Tris pH 7.5, 50 mM KCl, 1 mM DTT, 5% glycerol, 1 mM EDTA, 50 ng/µl polydI-dC (Sigma) and 50 ng/µl bovine serum albumin (New England Biolabs). Non-biotinylated competitor probes (wt or mutant A) were used at three concentrations: 200 fmole/µl, 50 fmole/µl or 10 fmole/µl (corresponding to 200, 50 and 10 fold more than biotinylated probe, respectively). Reactions were pre-incubated for 10 minutes at room temperature (~20 degrees Celsius). Next, 20 fmoles of biotinylated probe (1 fmole/µl; wtA or mutated A) was added, and incubated for 20 minutes at room temperature. To test for a supershift of the protein/DNA complex, 1ug of FLAG antibody (anti-mouse; Sigma) was added to the binding assay 10 minutes after the probe was added. Then, the reactions were loaded on a non-denaturing 5% acrylamide gel in 0.5x TBE buffer (Biorad). After transfer to a nylon hybond-N^+ membrane (GE Healthcare), the position of the biotinylated probes was identified using a streptavidin-horseradish peroxidase system (Pierce).

LHX6 and LHX8 proteins were generated by Fugene6 transfection of HEK 293 cells using expression vectors described above (see “plasmid vectors” section). All transfections with LHX6 or LHX8 also contained the LDB1 expression vector. After 48 hours, nuclear extracts were prepared using the Pierce nuclear extract kit. Protease inhibitor cocktail (Pierce) was used to prevent protein degradation; Expression of the proteins (LHX6, 3xFLAG-LHX8 and LDB1) in the different nuclear extracts were measured by western blot using rabbit anti-LHX6 (1/1000, Abcam), mouse anti-FLAG (1/2000, Sigma) and rabbit anti-LDB1 (1/1000, Dr. Heiner Westphal, NICHD) antibodies.

Biotinylated DNA probes: Probe A corresponded to the 26-64 bp of the SBE3 enhancer and included LHX site A (Fig. 8A; Probe A sequence delimited by the box; the LHX site A is in red and its core sequence is underlined; the TAATCA core is changed to TTTTTT in the mutant) (5'-TTTACAGGCCTGACAGATAATCAAGGCCTTA TTATACTG-3'). A mutated probe was used to test the specificity of Lhx6&8 binding to LHX site A; mutated probe A: 5'- TTTACAGGCCTGACAGATTTTTTAGGCCTTA TTATACTG -3'. Non-biotinylated probes were used in competition assays.

References

Choi, G.B., Dong, H.W., Murphy, A.J., Valenzuela, D.M., Yancopoulos, G.D., Swanson, L.W, and Anderson, D.J. (2005). Lhx6 delineates a pathway mediating innate reproductive behaviors from the amygdala to the hypothalamus. Neuron 46, 647-660.

Cobos I., Borello U., and Rubenstein J.L. (2007). Dlx transcription factors promote migration through repression of axon and dendrite growth. Neuron 54, 873–888.

Dassule, H.R., Lewis, P., Bei, M., Maas, R., and McMahon, A.P. (2000). Sonic hedgehog regulates growth and morphogenesis of the tooth. Development 127, 4775-4785.

Flandin, P., Kimura, S., and Rubenstein, J.L. (2010). The progenitor zone of the ventral medial ganglionic eminence requires nkx2-1 to generate most of the globus pallidus but few neocortical interneurons. J. Neurosci. 30, 2812-2823.

Gaspar-Maia, A., Alajem, A., Polesso, F., Sridharan, R., Mason, M.J., Heidersbach, A., Ramalho-Santos, J., McManus, M.T., Plath, K., Meshorer, E., and Ramalho-Santos, M. (2009). Chd1 regulates open chromatin and pluripotency of embryonic stem cells. Nature 460, 863-868.

Kimura, N., Ueno, M., Nakashima, K., and Taga, T. (1999). A brain region-specific gene product Lhx6.1 interacts with Ldb1 through tandem LIM-domains. J. Biochem. 126, 180-187.

Potter, G., Petryniak, M., Shevchenko, E., McKinsey, G., Ekker, M., and Rubenstein, J.L.R. (2009). Generation of Cre-transgenic mice using Dlx1/Dlx2 enhancers and their characterization in GABAergic interneurons. Molecular and Cellular Neuroscience. Mol. Cell Neurosci. 40, 167-186.

Scheffler, B., Walton, N.M., Lin, D.D., Goetz, A.K., Enikolopov, G., Roper, S.N., and Steindler, D.A. (2005). Phenotypic and functional characterization of adult brain neuropoiesis. Proc. Natl. Acad. Sci. U.S.A. 102, 9353-9358.

Shah, N.M., Pisapia, D.J., Maniatis, S., Mendelsohn, M.M., Nemes, A., and Axel, R. (2004). Visualizing sexual dimorphism in the brain. Neuron 43, 313–319.

Zhao, Y., Guo, Y.J., Tomac, A.C., Taylor, N.R., Grinberg, A. Lee, E.J., Huang, S., and Westphal, H. (1999). Isolated cleft palate in mice with a targeted mutation of the LIM homeobox gene lhx8. Proc Natl Acad Sci USA 96, 15002-6.